

# Double parameterized regularization inversion method for migration velocity analysis in transversely isotropic media with a vertical symmetry axis

Caixia Yu<sup>1,2</sup>, Yanfei Wang<sup>1\*</sup>, Jingtao Zhao<sup>1,2,3</sup> and Zhenli Wang<sup>1</sup>

<sup>1</sup>Key Laboratory of Petroleum Resources Research, Institute of Geology and Geophysics, Chinese Academy of Sciences, P.O. Box 9825, Beijing, 100029, P.R. China, <sup>2</sup>University of Chinese Academy of Sciences, Beijing, 100049, P.R. China, and <sup>3</sup>Research Institute of Petroleum Exploration & Development, PetroChina, Beijing, 100083, P.R. China

Received November 2012, revision accepted October 2013

## ABSTRACT

Simultaneous estimation of velocity gradients and anisotropic parameters from seismic reflection data is one of the main challenges in transversely isotropic media with a vertical symmetry axis migration velocity analysis. In migration velocity analysis, we usually construct the objective function using the  $l_2$  norm along with a linear conjugate gradient scheme to solve the inversion problem. Nevertheless, for seismic data this inversion scheme is not stable and may not converge in finite time. In order to ensure the uniform convergence of parameter inversion and improve the efficiency of migration velocity analysis, this paper develops a double parameterized regularization model and gives the corresponding algorithms. The model is based on the combination of the  $l_2$  norm and the non-smooth  $l_1$  norm. For solving such an inversion problem, the quasi-Newton method is utilized to make the iterative process stable, which can ensure the positive definiteness of the Hessian matrix. Numerical simulation indicates that this method allows fast convergence to the true model and simultaneously generates inversion results with a higher accuracy. Therefore, our proposed method is very promising for practical migration velocity analysis in anisotropic media.

**Key words:** VTI media, Migration velocity analysis, Double parameterized regularization, Quasi-Newton method.

## INTRODUCTION

Robust estimation of seismic velocities from reflection data plays an essential role in subsurface imaging and characteristic analysis of complex reservoirs (Alkhalifah and Tsvankin 1995; Alkhalifah 1997). Numerous examples demonstrate that application of prestack depth migration with anisotropic migration velocity analysis (MVA) for building a velocity model can yield significantly improved images (Berkhout 1997; Zhou, Guo and Young 2001; Li and Biondi 2011; Weibull and Arntsen 2012). Generally speaking, there are two feasible strategies for velocity estimation in the context of depth migration. The two strategies differ by the domain

in which the information is used to update the velocity model (Sava and Vlad 2008). The first strategy is formulated in the data space before migration, and it involves matching the recorded data with the simulated data obtained by using an approximate background velocity model. Lots of intensive and classic work about this strategy has been done. Based on synthesis of common focus point (CFP) gathers, Berkhout (1997) proposed a procedure for velocity analysis. Biloti, Santos and Tygel (2002) considered a velocity model inversion scheme by using common reflection surface (CRS) parameters. The second strategy is formulated in the image space after migration, and it involves measuring and correcting image features that indicate the model's inaccuracies. Techniques in this category are known as MVA. The initial work on MVA (Yilmaz and Chambers 1984) demonstrated the potential

\*E-mail: yfwang@mail.iggcas.ac.cn

of using common image gathers (CIGs) for the velocity inversion process. Liu and Bleistein (1995) analysed the properties of CIGs and derived analytic formulae to represent residual moveout in MVA. Alkhalifah (1995) developed a method of velocity analysis for transversely isotropic media based on the inversion of P-wave normal moveout (NMO) velocities with dip angle dependence. Zhou *et al.* (2001) proposed a tomographic method for MVA, where they solved linear equations to obtain the layer velocity and anisotropic parameters. Sarkar and Tsvankin (2003, 2004) presented a two-dimensional (2D) MVA algorithm designed to simultaneously estimate the spatially varying velocity along with the Thomsen parameters  $\varepsilon$  and  $\delta$  in factorized transversely isotropic media with a vertical symmetry axis (VTI) media. Charles *et al.* (2008) suggested a data-driven reflection tomography velocity model-building approach by using an automated global tomography method. Wang and Tsvankin (2011) advanced a P-wave tomographic algorithm for estimation of the symmetry-direction velocity and the anisotropic parameters  $\varepsilon$  and  $\delta$ .

However, unlike the types of isotropic velocity analysis (Stork 1992), the quality of anisotropic velocity analysis (Grechka and Tsvankin 1999; Tsvankin 2001; Woodward *et al.* 2008; Liu 2010; Li and Biondi 2011; Weibull and Arntsen 2012) suffers from the trade-offs between anisotropic parameters, velocity variation and reflecting interface dips. For practical applications, a typical way is to assume that the model is layered or blocked and then update the velocities and the Thomsen (1986) anisotropic parameters iteratively (Grechka, Pech and Tsvankin 2002; Behera and Tsvankin 2009). In this paper, our velocity analysis work is focused on factorized VTI media, which provides a convenient way of building vertically and laterally heterogeneous anisotropic models for prestack depth migration (Alkhalifah 1995; Sarkar and Tsvankin 2003, 2004).

In view of the inversion theory, MVA for seismic data is a non-linear inversion problem (Adler *et al.* 2008) which can be solved by iterative application of migration and velocity updating. Costa *et al.* (2008) introduced a regularization scheme for slope tomography by using reflection-angle-based smoothness as a constraint and compared the effects with three other conventional constraints. The smoothness constraint has a distinct effect on the velocity model but a weak effect on migrated data, thus leading to geologically more consistent models. To estimate the optimum earth velocity model, people usually minimize a user-defined residual image. This corresponds to the construction of an objective function according to the  $l_2$  norm, and the linear conjugate gradient scheme is used to solve

such an inversion problem. However, the inversion result may be unstable and non-unique (Zhang and Yang 2003; Wang, Yang and Duan 2009). In addition, MVA is a very time-consuming process in seismic data inversion. Therefore, it is necessary to optimize the objective function to reduce the non-uniqueness and improve the efficiency of velocity updating.

We study the double parameterized regularization inversion method for MVA in factorized VTI media. This method combines the benefits of the  $l_2$  norm and the  $l_1$  norm, which fits the real data using the  $l_2$  norm and reduces the non-uniqueness and outliers by the  $l_1$  norm constraint. The reason for proposing double parameterized regularization is that the horizontal and vertical velocity gradients and the unknown anisotropic parameters may possess non-smoothing information as they cross the boundaries of the layers or blocks. A double parameterized regularization algorithm can ensure the uniform convergence of anisotropic media parameter inversion, and thus reduce iteration numbers during the process of MVA. In this way, efficiency of MVA can be highly improved.

## METHODOLOGY

### Migration velocity analysis

Sarkar and Tsvankin (2004) introduced a migration velocity analysis algorithm specially designed for piecewise-factorized VTI media, which includes the following four main steps:

1. Use prestack depth migration with an initial estimation of medium parameters to create an image of the subsurface.
2. Pick reflectors in each VTI block to delineate the reflector shapes on the migrated section.
3. Use semblance scanning to evaluate the residual moveout of reflection events in CIGs.
4. Update the medium parameters prepared for the next application of prestack depth migration.

Repeat the above four steps until the events in the image gathers become sufficiently flat.

### Model parameterization

The algorithm for P-wave MVA is designed for geological models composed of factorized VTI layers or blocks with a linear velocity function  $V_{P0}(x, z)$ :

$$V_{P0}(x, z) = V_{P0}(x_0, z_0) + k_x(x - x_0) + k_z(z - z_0), \quad (1)$$

where  $V_{P0}(x_0, z_0)$  is the value at a specific point  $(x_0, z_0)$ ,  $k_x$  and  $k_z$  are horizontal and vertical velocity gradients, respectively.

Using common sense, depth imaging of P-wave data requires the knowledge of five parameters ( $V_{P0}$ ,  $k_x$ ,  $k_z$ ,  $\varepsilon$  and  $\delta$ ) in each layer or block.

Table 1 Parameters of the VTI media model.

Parameters	$V_{P0}(0,0)$ (m/s)	$k_x$ ( $s^{-1}$ )	$k_z$ ( $s^{-1}$ )	$\varepsilon$	$\delta$
Accurate values	2000	0.200	0.600	0.300	0.100
Initial values	2000	0.100	0.300	0.000	0.000

P-wave space-time domain signatures in VTI media are fully controlled by the NMO velocity and the anellipticity coefficient  $\eta$ , and are independent of the vertical velocity (Alkhalifah, Fomel and Biondi 2001). Sarkar and Tsvankin (2004) showed that for models without significantly changing dips above the target layer, the moveout of events in CIGs is governed by the following four combined parameters:

1. The NMO velocity at a certain point on the surface of each factorized layer or block,  $V_{nmo} = V_{P0}\sqrt{1+2\delta}$ .
2. The vertical velocity gradient,  $k_z$ .
3. The modified lateral velocity gradient combined with the parameter  $\delta$ ,  $\hat{k}_x = k_x\sqrt{1+2\delta}$ .
4. The anellipticity parameter,  $\eta = \frac{\varepsilon-\delta}{1+2\delta}$ .

In their assumption, the velocity  $V_{P0}$  has to be known at a certain point within the factorized layers or blocks to decouple the horizontal gradient  $k_x$  from the coefficient  $\delta$  and to determine another anisotropic coefficient  $\varepsilon$  (Tsvankin and Thomsen 1994; Sarkar and Tsvankin 2003).

### Residual moveout equation

Sarkar and Tsvankin (2004) estimated the vertical velocity gradient  $k_z$  using two reflectors located at different depths in each factorized layer or block. To constrain the parameter  $\eta$  (and therefore  $\varepsilon$  and  $\delta$ ), the residual moveout in CIGs is described by the following non-hyperbolic equation:

$$z_M^2(b) \approx z_M^2(0) + r_1 b^2 + r_2 \frac{b^4}{b^2 + z_M^2(0)}, \quad (2)$$

where  $z_M$  is the migrated depth and  $b$  is the half-offset. The coefficients  $r_1$  and  $r_2$ , which quantify the magnitude of residual moveout, are estimated by 2D semblance scanning. The goal of the iterative MVA algorithm is to make events in CIGs flatten by minimizing coefficients  $r_1$  and  $r_2$ . The coefficient  $r_2$  has great sensitivity to the parameter  $\eta$ , which assumes responsibility for non-hyperbolic moveout at long offsets.

### Double parameterized regularization model

To simplify a general non-linear inverse (minimization) problem, we perform the MVA iteratively. Assuming that some

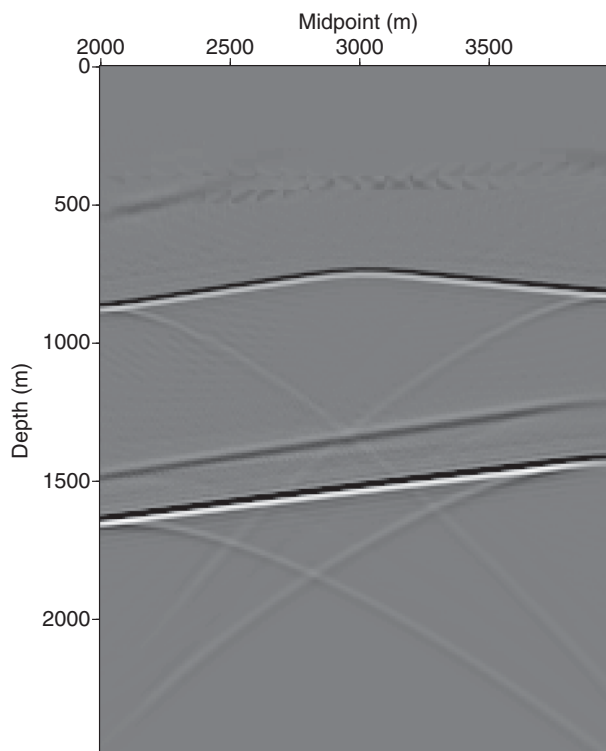


Figure 1 Prestack depth migration image with the initial model parameters.

iterations of MVA have been implemented, the prestack depth migration produces the migrated depths  $z_0(x_j, b_k)$ , ( $x_j$  is the midpoint of the  $j$ -th image gather,  $b_k$  is the half-offset), and  $\hat{z}(x_j) = (1/M) \sum_{k=1}^M z_0(x_j, b_k)$  is the average migrated depth of a reflection event with  $M$  the number of offsets in each image gather.

We iteratively update the parameter vector  $\lambda$  (its elements are  $k_x$ ,  $k_z$ ,  $\varepsilon$  and  $\delta$ ) by minimizing the following objective function using a double parameterized regularization model:

$$J^{\alpha,\beta}(\Delta\lambda) = \frac{1}{2} \|\mathbf{A}\Delta\lambda + \mathbf{b}\|^2 + \frac{\beta}{2} \|\Delta\lambda - \Delta\lambda^0\|^2 + \alpha\Omega(\Delta\lambda), \quad (3)$$

where  $\mathbf{A}$  is a matrix with  $M \times P$  rows ( $P$  is the number of image gathers used for velocity updating) and  $N$  columns whose elements are the derivatives of the migrated depths with respect to the medium parameters  $[\partial z_0(x_j, b_k)/\partial \lambda_i]$  and  $\mathbf{b}$  is a vector with  $M \times P$  elements defined by  $z_0(x_j, b_k) - \hat{z}_0(x_j)$ . The model-update  $\Delta\lambda$  is a vector,  $\Delta\lambda^0$  is the initial guess vector of medium parameters, and  $\alpha$  and  $\beta$  are regularization parameters. In each step of MVA, the parameter vector  $\lambda$  is updated by

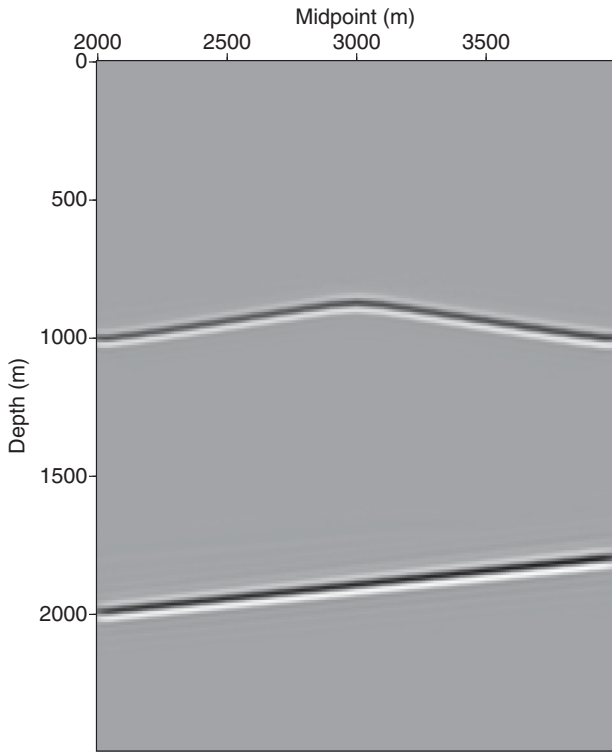


Figure 2 Prestack depth migration image with the actual model parameters.

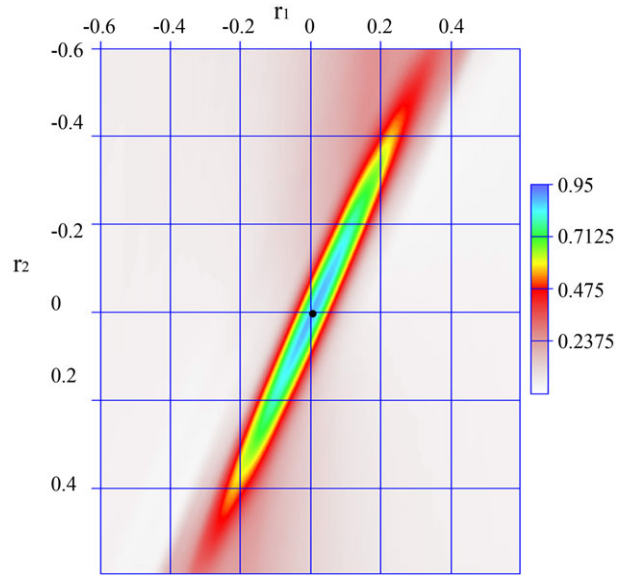


Figure 4 Semblance scan for the first reflector after seven iterations; the lateral coordinate is 3 km.

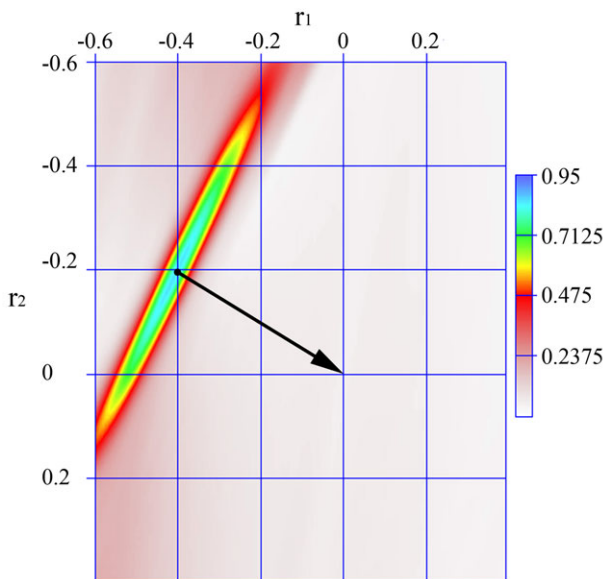


Figure 3 Semblance scan for the first reflector in the initial model; the lateral coordinate is 3 km.

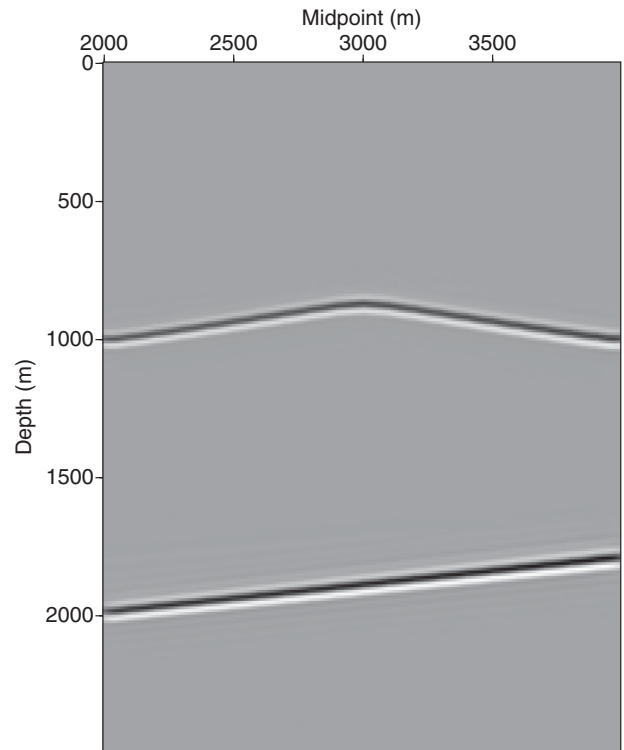


Figure 5 Stacked image for the model after seven iterations using the double parameterized regularization method.

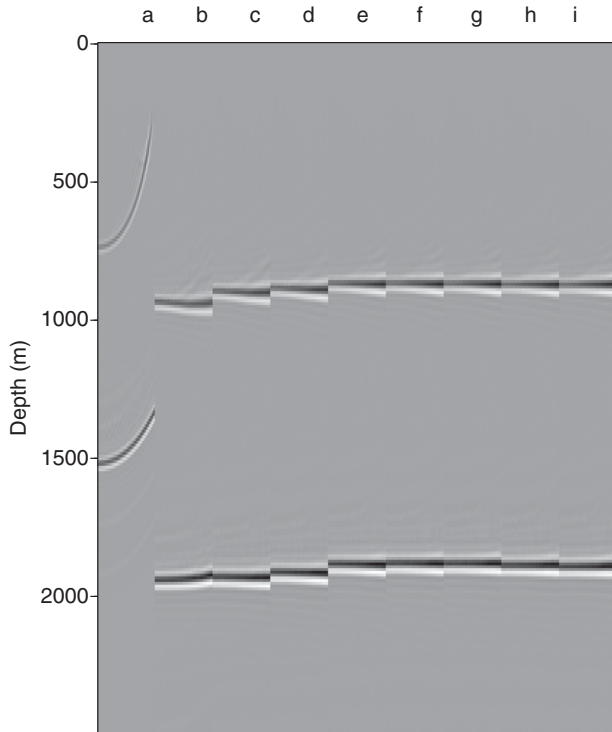


Figure 6 Residual moveout in image gathers for both reflectors in the model at the surface location 3km: (a) for the initial model; (b) after one, (c) two, (d) three, (e) four, (f) five, (g) six and (h) seven iterations, (i) for the true model.

an initial value of  $\lambda$  plus  $\Delta\lambda$ . The non-smooth function  $\Omega(\Delta\lambda)$  is defined as a Huber norm function (Wang *et al.* 2011a):

$$\Omega(\Delta\lambda) = \sum_i h_{\tilde{\varepsilon}}(\Delta\lambda_i),$$

where  $h_{\tilde{\varepsilon}}(\cdot)$  is defined as a non-linear piecewise function

$$h_{\tilde{\varepsilon}}(x) = \begin{cases} \frac{x^2}{2\tilde{\varepsilon}}, & 0 \leq x \leq \tilde{\varepsilon}, \\ x - \frac{\tilde{\varepsilon}}{2}, & x > \tilde{\varepsilon} > 0, \\ -x - \frac{\tilde{\varepsilon}}{2}, & -x < -\tilde{\varepsilon} < 0, \end{cases}$$

and  $\tilde{\varepsilon}$  is a small constant parameter. Clearly, as  $\tilde{\varepsilon} \rightarrow 0$   $\Omega(\Delta\lambda)$  approximates the  $l_1$  norm very well.

**Quasi-Newton method**

Supposing  $\mathbf{H}(\Delta\lambda)$  is the Hessian matrix of the function  $J^{\alpha,\beta}(\Delta\lambda)$ , we use its approximation value instead of the explicit formula of  $\mathbf{H}(\Delta\lambda)$ . In the optimization community,

Table 2 Inversion results of MVA in VTI media.

Methods	Iterative				
	numbers	$k_x(s^{-1})$	$k_z(s^{-1})$	$\varepsilon$	$\delta$
Double regularization	7	0.199202	0.594767	0.306139	0.108021
$\alpha = 0, \beta \neq 0$	12	0.198259	0.591786	0.309300	0.108622
$\beta = 0, \alpha \neq 0$	11	0.197690	0.586840	0.310857	0.111154

Table 3 Inversion errors of MVA in VTI media.

Methods	Iterative numbers	$k_x$	$k_z$	$\varepsilon$	$\delta$
		error (%)	error (%)	error (%)	error (%)
Double regularization	7	-0.399	-0.872	2.046	8.021
$\alpha = 0, \beta \neq 0$	12	-0.871	-1.369	3.100	8.622
$\beta = 0, \alpha \neq 0$	11	-1.155	-2.193	3.619	11.154

quasi-Newton methods can be used to solve the non-linear and non-quadratic minimization problems. The essence is using correction formulae to ensure the positive definiteness of the approximate Hessian matrix. Generally speaking, Newton’s method needs the second-order partial derivatives to be calculated, while the quasi-Newton method only requires the first-order partial derivatives to ensure fast convergence (Yuan and Sun 1997). Therefore, we use the quasi-Newton method to solve our minimization problem (Appendix).

The gradient of the function  $J^{\alpha,\beta}(\Delta\lambda)$  with respect to medium parameters is as follows:

$$g(\Delta\lambda) = \mathbf{A}^T(\mathbf{A}\Delta\lambda + \mathbf{b}) + \alpha K(\Delta\lambda) + \beta(\Delta\lambda - \Delta\lambda^0), \tag{4}$$

where the function  $K(\Delta\lambda)$  is defined as:

$$K(\Delta\lambda) = \left[ \frac{\partial\Omega}{\partial\Delta\lambda_1}, \dots, \frac{\partial\Omega}{\partial\Delta\lambda_p} \right]^T,$$

and  $\frac{\partial\Omega}{\partial\Delta\lambda_i} = \sum_i h'_{\tilde{\varepsilon}}(\Delta\lambda_i)$ , the derivative of  $h_{\tilde{\varepsilon}}(x)$ , is given by

$$h'_{\tilde{\varepsilon}}(x) = \begin{cases} \frac{x}{\tilde{\varepsilon}}, & 0 \leq x \leq \tilde{\varepsilon}, \\ 1, & x > \tilde{\varepsilon} > 0, \\ -1, & -x < -\tilde{\varepsilon} < 0. \end{cases}$$

Supposing  $\mathbf{B} \approx \mathbf{H}^{-1}(\Delta\lambda)$ , the gradient of the function  $J^{\alpha,\beta}(\Delta\lambda)$  in the  $k$ -th iteration is defined as  $\mathbf{g}_k = g(\Delta\lambda_k)$ , and the direction for updating medium parameters is defined as  $\mathbf{s}_k = (\Delta\lambda)_{k+1} - (\Delta\lambda)_k$ . Therefore, the next model parameters

Table 4 Parameters of the fault model.

Parameters	$V_{p0}(0,0)(\text{m/s})$	$k_x (s^{-1})$	$k_z (s^{-1})$	$\varepsilon$	$\delta$
Accurate values	2100	0.100	0.500	0.200	0.100
Initial values	2100	0.000	0.000	0.000	0.000

can be updated using the following equations (Wang, Yagola and Yang 2011b):

$$\begin{cases} (\Delta\lambda)_{k+1} = (\Delta\lambda)_k + \omega_k \mathbf{d}_k, \\ \mathbf{d}_k = -\mathbf{B}_k \mathbf{g}_k, \end{cases}$$

where the matrix  $\mathbf{B}_k$  is calculated using the following formulae:

$$\begin{cases} \mathbf{B}_{k+1} = \mathbf{V}_k^T \mathbf{B}_k \mathbf{V}_k + \rho_k \mathbf{s}_k \mathbf{s}_k^T, \\ \rho_k = \frac{1}{\mathbf{y}_k^T \mathbf{s}_k}, \\ \mathbf{V}_k = \mathbf{I} - \rho_k \mathbf{y}_k \mathbf{s}_k^T, \\ \mathbf{y}_k = \mathbf{g}_{k+1} - \mathbf{g}_k. \end{cases} \quad (5)$$

The parameter  $\omega_k$  is the step size, which can be obtained by the Wolfe line search criterion, i.e. the parameter  $\omega_k$  should satisfy the following two conditions (Yuan and Sun 1997):

$$J^{\alpha,\beta}(\Delta\lambda_k + \omega_k \mathbf{d}_k) \leq J^{\alpha,\beta}(\Delta\lambda_k) + r \omega_k \mathbf{g}_k^T \mathbf{d}_k, \quad (6)$$

$$\mathbf{d}_k^T \mathbf{g}_{k+1} \geq \tilde{r} \mathbf{d}_k^T \mathbf{g}_k, \quad (7)$$

where  $r$  and  $\tilde{r}$  are two constant numbers requiring  $0 < r < \tilde{r} < 1$ . In our numerical experiments, we fix values of  $r$  as 0.1 and  $\tilde{r}$  as 0.4.

The inversion algorithm flow chart can be described as follows.

**Step 1.** Use initial medium parameters  $\Delta\lambda_0$ , a constant parameter  $r$  and a symmetric positive definite matrix  $\mathbf{B}_0$  ( $\mathbf{B}_0$  can be an identity matrix), and set  $k = 0$ .

**Step 2.** Compute  $g(\Delta\lambda_k)$ . If  $\|g(\Delta\lambda_k)\| < \xi \cdot \max\{1, \|g(\Delta\lambda_0)\|\}$  (where  $\xi < 0.1$ ), STOP; otherwise, GOTO Step 3.

**Step 3.** Compute  $\begin{cases} \mathbf{d}_k = -\mathbf{B}_k \mathbf{g}_k, \\ \Delta\lambda_{k+1} = \Delta\lambda_k + \omega_k \mathbf{d}_k, \end{cases}$  where  $\omega_k$  satisfies equations (6) and (7).

**Step 4.** Set  $k = k + 1$ , and update  $\mathbf{B}_k$  by formulae (5); GOTO Step 2.

**Remark 1** In practical applications, the inversion algorithm can be realized with limited-memory storage by formulae (5) to build the updating matrix. This can be clearly seen from the following equation:

$$\begin{aligned} \mathbf{B}_{k+1} &= (\mathbf{V}_k^T \mathbf{V}_{k-1}^T \cdots \mathbf{V}_{k-\hat{m}}^T) \mathbf{B}_0 (\mathbf{V}_{k-\hat{m}} \cdots \mathbf{V}_{k-1} \mathbf{V}_k) \\ &+ \rho_{k-\hat{m}} (\mathbf{V}_k^T \mathbf{V}_{k-1}^T \cdots \mathbf{V}_{k-\hat{m}+1}^T) \mathbf{s}_{k-\hat{m}} \mathbf{s}_{k-\hat{m}}^T (\mathbf{V}_{k-\hat{m}+1} \cdots \mathbf{V}_{k-1} \mathbf{V}_k) \end{aligned}$$

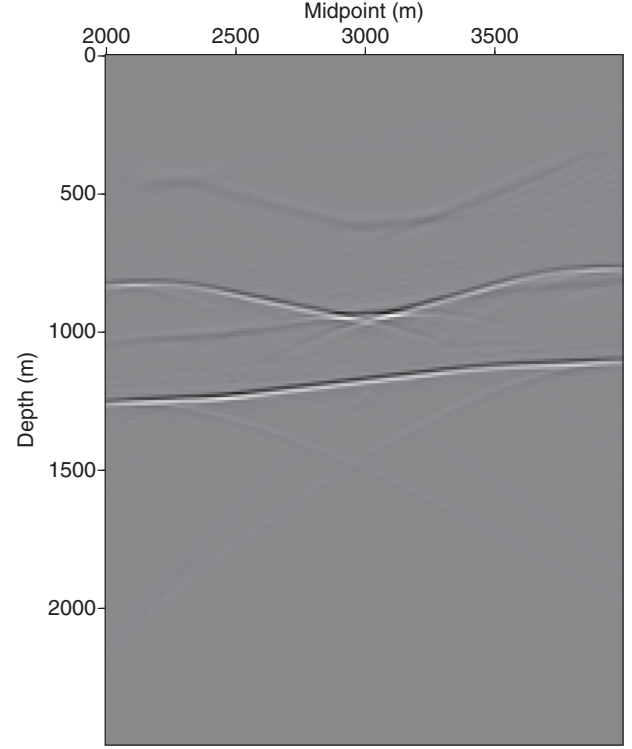


Figure 7 Prestack depth migration image with the initial fault model parameters.

$$\begin{aligned} &+ \rho_{k-\hat{m}+1} (\mathbf{V}_k^T \mathbf{V}_{k-1}^T \cdots \mathbf{V}_{k-\hat{m}+2}^T) \mathbf{s}_{k-\hat{m}+1} \mathbf{s}_{k-\hat{m}+1}^T \\ &\times (\mathbf{V}_{k-\hat{m}+2} \cdots \mathbf{V}_{k-1} \mathbf{V}_k) + \cdots + \rho_k \mathbf{s}_k \mathbf{s}_k^T. \end{aligned}$$

Therefore, the algorithm can be fast realized in computation only by storing  $\mathbf{s}_i$ ,  $\mathbf{y}_i$  in practical calculations.

**Remark 2** Stopping criteria is a key issue for an inversion algorithm. For general inverse problems, there exists a ‘saturation’ state of approximation for the iterative algorithm, which means that the magnitude of the error of a solution must be in agreement with the accuracy of the assignment of the input data (Wang 2007). So a proper stopping criterion is needed. If we consider the conventional gradient energy value as the stopping criterion, it will fall into too many iterations and lead to the accumulation of computing errors. Therefore, we choose ‘if  $\|g(\Delta\lambda_k)\| < \xi \cdot \max\{1, \|g(\Delta\lambda_0)\|\}$  is satisfied, then we terminate the iteration’ as the stopping criterion, where  $\xi$  is a user-controlled parameter and  $\xi < 0.1$  is usually required. Of course, this choice of stopping criterion is not optimal. In the inversion community, other stopping rules may be applied, for example using the norm of the discrepancy between the data and its approximate values.

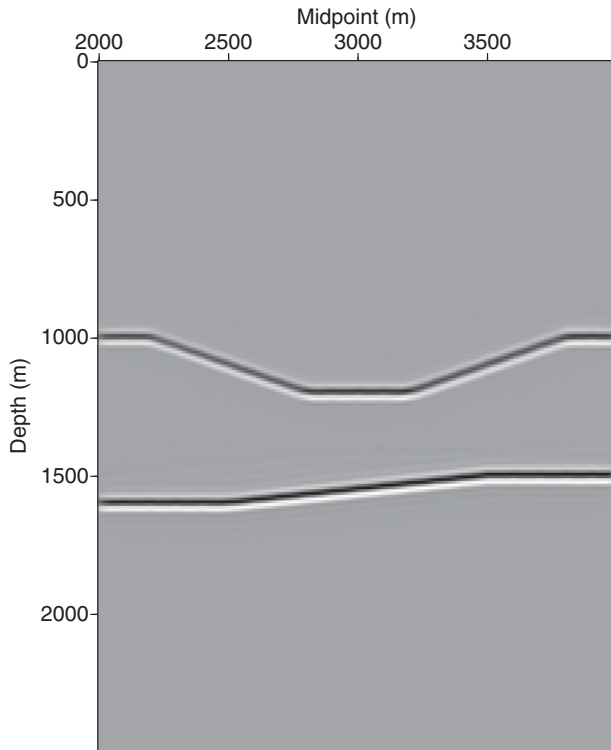


Figure 8 True image of the fault model obtained by anisotropic prestack depth migration with the true medium parameters.

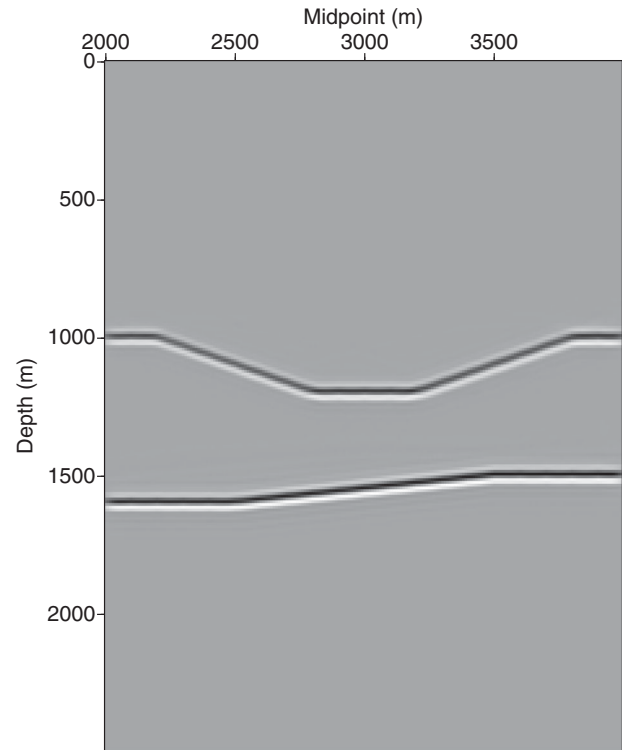


Figure 9 Stacked image for the fault model after seven iterations using the double parameterized regularization method.

### The principles of choosing regularization parameters

Regularization parameters  $\alpha$  and  $\beta$  in the objective function (equation (3)) play a key role in inversion implementation. Principles of choosing suitable regularization parameters can be given as follows:

1. If  $\alpha = 0, \beta > 0$ , the objective function (equation (3)) will degenerate into a smoothly controlled regularization model. And if  $\beta$  is chosen beyond the range of the anisotropic medium's parameter values (e.g.  $\beta$  is too large), then inaccurate inversion results will occur. Of course, this case will rarely appear, as long as prior information is considered.
2. If  $\beta = 0, \alpha > 0$ , we will obtain a non-smoothly controlled regularization model from the objective function (equation (3)). Apparently, if  $\alpha$  is too large, the minimization problem will be transformed into a model primarily characterized by a non-smooth property. In such a case, the solution of the inverse problem is usually not unique, and some additional constraints must be adopted to determine a suitable result.
3. If  $\alpha > 0, \beta > 0$ , the optimal inversion results can be obtained by choosing parameters  $\alpha$  and  $\beta$  properly. We notice that  $k_x$  and  $k_z$  are the horizontal and vertical velocity gradients, respectively, and  $\varepsilon$  and  $\delta$  are the unknown anisotropic param-

eters in the factorized VTI media model; therefore, a double regularization parameters algorithm can provide more accurate inversion results of media model parameters than the single regularization parameters algorithm.

In numerical calculations, we choose the regularization parameters  $\alpha$  and  $\beta$  according to the Tikhonov regularization theory. As the values of  $\alpha$  and  $\beta$  tend to 0 but are greater than 0, the inversion parameters will be close to the true values. Therefore, we choose  $\alpha$  and  $\beta$  in an *a priori* way:  $0 < \beta < \alpha < 0.1$ .

## NUMERICAL EXPERIMENTS

### Factorized VTI layer with smooth interface

First, we consider two smooth reflectors embedded in a factorized VTI media with a linear variation velocity. The anisotropic parameters  $\varepsilon, \delta$  are taken to be constant values. The SUSYNLVANTI code in Seismic Unix (SU) is utilized to make synthetic common shot records, with shot interval equalling 50 m, trace interval equalling 50 m and number of traces, 40. Number of the time sample is taken as 1000 with a sampling interval of 4 ms. The Ricker wavelet with a

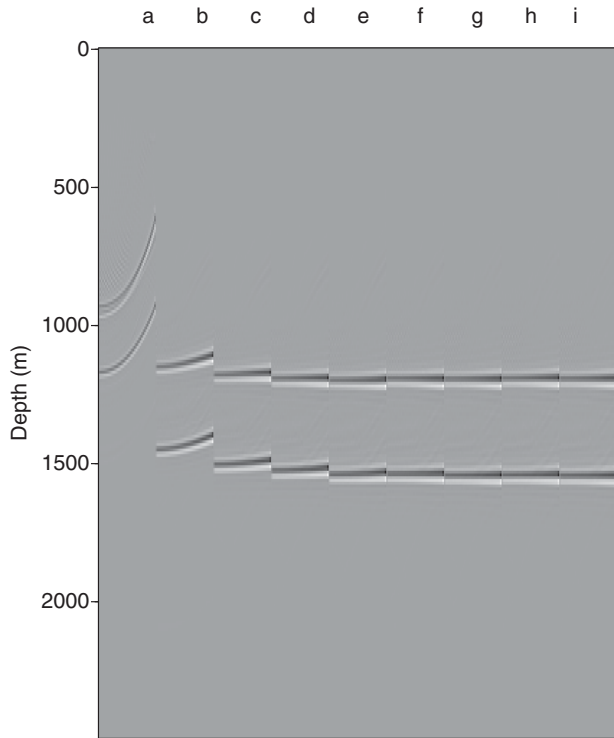


Figure 10 Residual moveout in image gathers for both reflectors in the fault model at the surface location 3km: (a) for the initial model; (b) after one, (c) two, (d) three, (e) four, (f) five, (g) six and (h) seven iterations, (i) for the true model.

Table 5 Inversion results of MVA for fault model.

Methods	Iterative numbers	$k_x(s^{-1})$	$k_z(s^{-1})$	$\epsilon$	$\delta$
Double regularization	7	0.100580	0.492163	0.207252	0.097006
$\alpha = 0, \beta \neq 0$	12	0.103151	0.514373	0.204577	0.083205
$\beta = 0, \alpha \neq 0$	10	0.097445	0.509139	0.222591	0.095361

predominant frequency of 30 Hz is utilized. In the procedure of carrying out MVA, horizontal imaging coordinates ranging from 2 to 4 km are used to produce CIGs.

*Prestack depth migration*

Prestack depth migration has a great advantage in imaging problems of complex media (Liu 1997). Residual depth moveout in CIG has high sensitivity to model parameters, which makes prestack depth migration a powerful tool for velocity analysis. The initial model in MVA is supposed to use an

Table 6 Inversion errors of MVA for fault model.

Methods	Iterative numbers	$k_x$ error (%)	$k_z$ error (%)	$\epsilon$ error (%)	$\delta$ error (%)
Double regularization	7	0.580	-1.567	3.626	-2.994
$\alpha = 0, \beta \neq 0$	12	3.151	2.875	2.289	-16.795
$\beta = 0, \alpha \neq 0$	10	-2.555	1.828	11.296	-4.639

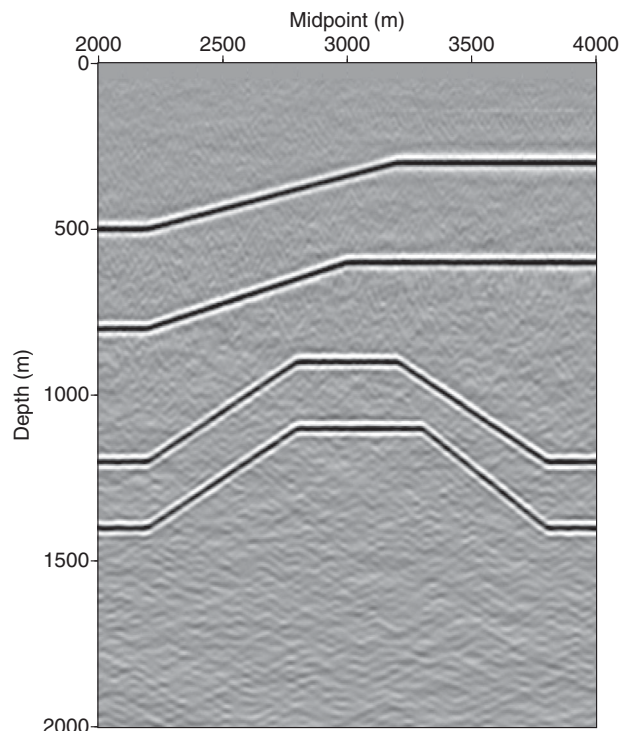


Figure 11 True image of the anticline model obtained by anisotropic prestack depth migration with the actual medium parameters.

isotropic medium. Through well data, velocity at some position on the surface is known in advance as  $V_{p0}(0, 0) = 2000$  m/s, as shown in Table 1. The prestack depth migration result is illustrated in Fig. 1. In order to explain how model parameters influence the results of the prestack depth migration, the imaging section with accurate model parameters is shown in Fig. 2. Comparison between Figs 1 and 2 indicates that an inaccurate elastic modulus has a direct effect on the focusing of the migration wave field, especially in the positioning of reflectors.



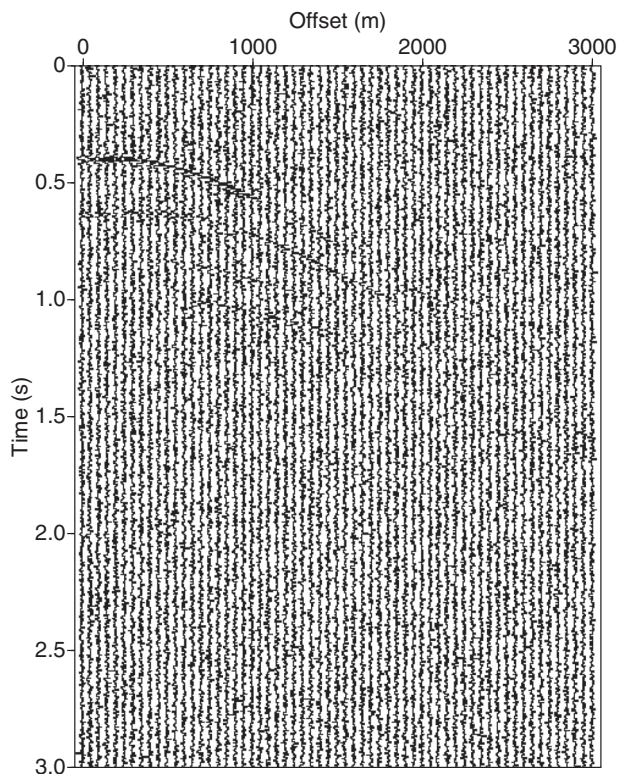


Figure 12 One of the noise-contaminated shot gathers (the lateral coordinate is close to 3 km).

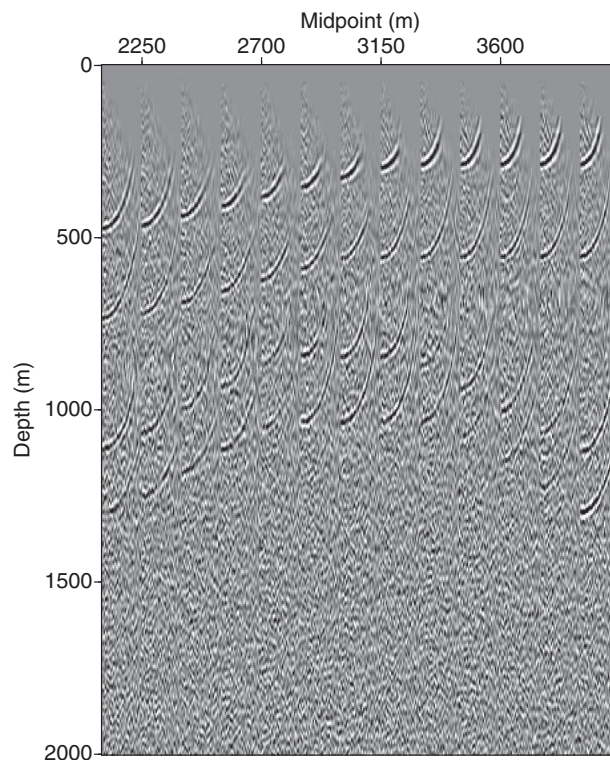


Figure 13 Image gathers for the anticline model obtained with the homogeneous, isotropic initial model.

Table 7 Parameters of the anticline model.

Parameters	$V_{P0}(x_0, z_0)$ (m/s)	$k_x$ ( $s^{-1}$ )	$k_z$ ( $s^{-1}$ )	$\varepsilon$	$\delta$
Accurate values	2000	0.02	0.50	0.00	0.00
Accurate values	2350	0.05	0.30	0.10	0.08
Initial values	2000	0.00	0.00	0.00	0.00
Initial values	2350	0.00	0.00	0.00	0.00

*Migration velocity analysis*

Now we present the parameter inversion process of this numerical simulation example using the proposed method.

*Picking curves of reflectors*

Curves of migration reflectors are picked on the prestack depth imaging section of the initial model, as displayed in Fig. 1, which will be taken as input data for inversion of  $z_M(0)$ , reflector dips and other parameters.

*Fitting curves of residual depth moveout*

According to the residual depth moveout equation (equation (2)), a semblance scanning method is used to ob-

tain the energy spectra of  $r_1$  and  $r_2$  for each reflector, as shown in Fig. 3. Through picking the best energy focusing point in energy spectra, optimal values of  $r_1$  and  $r_2$  will be obtained, which are other inputs for parameter inversion. Attention should be paid to the fact that although  $r_1$  and  $r_2$  couple with each other, both of them will tend to zero with iterations of MVA (see Figs 3 and 4). This phenomenon can be easily seen from equation (2).

*Updating model parameters*

The stacked image after seven iterations illustrates improvements in focusing and positioning of the two reflectors during the velocity updating. Events in CIG are flattened, and  $r_1$  and  $r_2$  tend to zero, which can be seen in Fig. 5.

In order to make the convergence process more visible, especially for event changes in CIG, a gather including two reflectors at 3 km position is illustrated in Fig. 6. In this figure, migration results with the initial model (furthest left), the model after seven iterations, and the true model (furthest right) are given. Figure 6 vividly illustrates that events in the image gather gradually tend to be flattened, with residual moveout converging to zero. After the sixth iteration, although events

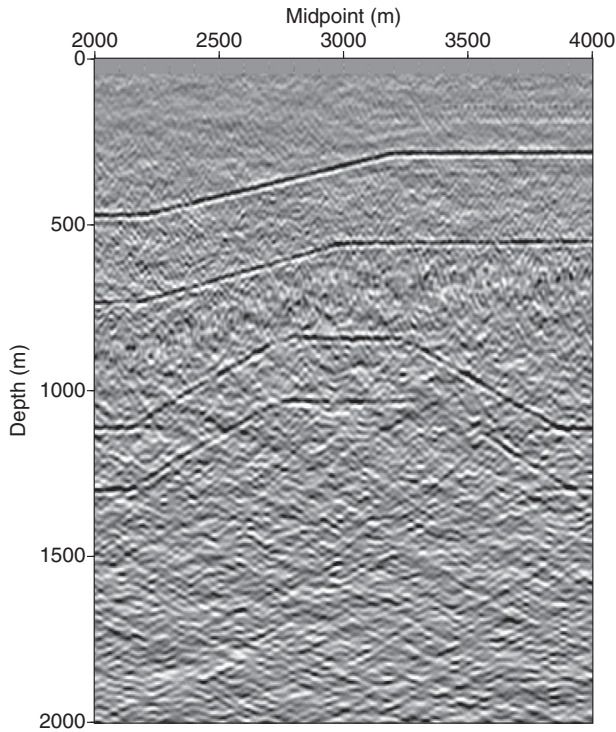


Figure 14 Prestack depth migration image with the initial anticline model parameters.

in CIG are flat and energy spectra of  $r_1$  and  $r_2$  are basically zero, the seventh iteration is still done and chosen as the final result, just for the sake of model convergence.

Table 2 illustrates the inversion results of the proposed double parameterized regularization method and the single parameterized regularization method ( $\alpha = 0$  or  $\beta = 0$  in the objective function). Iteration numbers verify that the double parameterized regularization inversion algorithm converges to the true model faster than the single parameterized regularization MVA algorithm. The proposed method dramatically improves the efficiency of the MVA, which shows great possi-

bility of potential applications for three-dimensional (3D) high density survey. Table 3 demonstrates another merit of the double parameterized regularization method, which can reduce errors of anisotropic parameters to a smaller degree and highly improve convergence accuracy of the objective function. This phenomenon can be confirmed from the fact that the double parameterized regularization method is built on a more elaborate model which supplies sufficient constraints to inversion parameters with both smoothness and non-smoothness. Also, the quasi-Newton correction formulation can always secure the positive definiteness of the Hessian matrix, which makes the iteration process more stable.

### Fault layers model

In our second synthetic example, the geology mode is designed to be a fault layered model with two reflectors in a factorized VTI half space. Kirchhoff prestack depth migration with the actual model parameters generates an accurate image of all reflectors, which is shown in Fig. 8. For the MVA, we use image gathers located between 2 and 4 km, with the maximum offset-to-depth ratio close to two. The velocity is assumed to be known at one location  $V_{P0}(0, 0) = 2100$  m/s and the parameters  $k_x$ ,  $k_z$ ,  $\varepsilon$  and  $\delta$  are to be updated. For field applications,  $V_{P0}$  can be obtained from checking shots or sonic logs acquired in a vertical borehole. The initial model consists of homogeneous and isotropic layers. Image gathers obtained with the initial model parameters (in Table 4) exhibit substantial residual moveout, which is demonstrated in Fig. 10. Kirchhoff prestack depth migration with initial model parameters is illustrated in Fig. 7. After seven iterations, the residual moveout for all reflectors is practically eliminated, and the reflectors are properly positioned (Fig. 9). Comparing Fig. 9 with Fig. 7 reveals that our proposed method exhibits great improvements in both focusing and positioning of reflectors. The magnitudes of the residual moveout for both reflectors are

Table 8 Inversion results of MVA for anticline model.

	Methods	Iterative numbers	$k_x(s^{-1})$	$k_z(s^{-1})$	$\varepsilon$	$\delta$
Layer 1	Double regularization	7	0.019643	0.490261	0.002041	0.001822
	$\alpha = 0, \beta \neq 0$	7	0.018838	0.474572	0.003370	0.003260
	$\beta = 0, \alpha \neq 0$	7	0.016712	0.467559	0.004359	0.005972
Layer 2	Double regularization	9	0.045406	0.305689	0.108418	0.066282
	$\alpha = 0, \beta \neq 0$	9	0.040491	0.312740	0.109783	0.052037
	$\alpha = 0, \beta \neq 0$	9	0.053321	0.346568	0.106118	0.056865

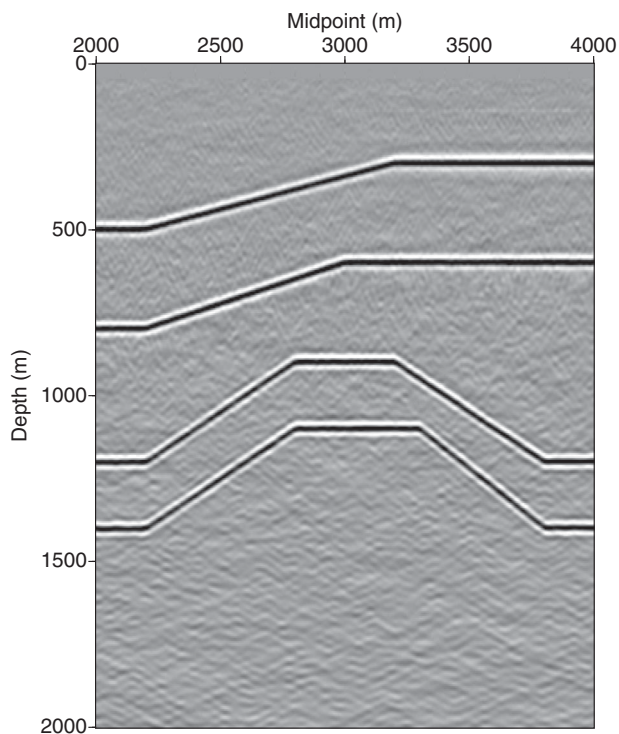


**Figure 15** Prestack depth migration image for the anticline model with the inverted parameters using our double parameterized regularization method.

convergent to their actual values, and events in image gather gradually tend to be flattened (see Fig. 10).

Table 5 shows that the inversion parameters are much closer to the correct values using the double parameterized regularization method. Furthermore, errors of anisotropic parameters are smaller using our proposed method than that of the single parameterized regulation method (see Table 6). Simulation results of the example demonstrate efficiency and reliability of our proposed double parameterized regulation method in MVA.

### Anticline model

Finally, we apply the algorithm to a VTI anticline model with dips up to  $30^\circ$  under an isotropic layer. The isotropic layer and the VTI layer are both vertically and laterally heterogeneous. Each layer contains two reflecting interfaces, as required by the MVA algorithm, with every second reflector serving as the boundary between layers. Anisotropic prestack depth migration with the correct model parameters (Table 7) for all layers is shown in Fig. 11. To assess the stability of our algorithms, we add random uncorrelated Gaussian noise to the synthetic

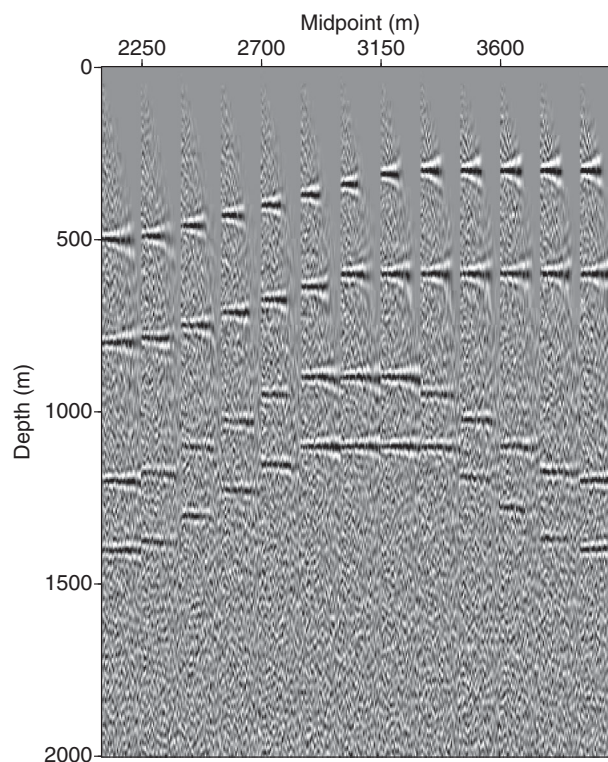


**Figure 16** Image gathers for the anticline model obtained using our double parameterized regularization method (Table 8).

data as shown in Fig. 12. We apply our MVA algorithm to ten image gathers located at horizontal coordinates ranging from 2 to 4 km with a maximum offset of 3 km. The medium parameters are estimated using a layer-stripping strategy starting at the surface.

The initial velocity model (Table 7) used in the first iteration of MVA is homogeneous and isotropic. For the first layer, the velocity  $V_{P0}$  is assumed to be known at a single surface location  $V_{P0}(3000, 0) = 2000$  m/s. We carry out parameter estimation for the second layer using the correct value of the vertical velocity at this point  $V_{P0}(3000, 600) = 2350$  m/s. Because the initial model parameters are strongly deviated from the true values, the events exhibit significant residual moveout (Fig. 13) and the depth of migration image is inaccurate (Fig. 14). With our double parameterized regularization method, the inverted parameters (Table 8) are close to the true values in all layers, and the migrated image (Fig. 15) is practically improved in both focusing and positioning of reflectors. After several iterative implementations of the prestack depth migration and velocity updating, all events in CIGs become sufficiently flat (Fig. 16).

With the same number of iterations for all three types of regularization methods, the inversion parameters are much closer to the correct values using our double parameterized regularization method than the results of single parameterized regularization methods (see Table 8).

## CONCLUSION

We designed a double parameterized regularization inversion method for MVA in a factorized VTI medium. Compared with the single parameterized regularization method, our double parameterized regularization method can dramatically reduce iteration numbers of MVA, and thus improve the efficiency of velocity model updating. The inversion errors of anisotropic parameters decrease more using the proposed double parameterized regularization method than with the single parameterized regularization method. In pursuing our algorithm's stability in inverting velocity model parameters, a quasi-Newton method is adopted to ensure the positive definiteness of the Hessian matrix during iterations. In particular, the double parameterized regularization inversion algorithm is not limited to factorized VTI velocity model inversion problems, which in theory can be extended to other geophysical inversion problems as long as a proper objective function can be constructed. In choosing regularization parameters  $\alpha$  and  $\beta$  for field applications, additional information has to be provided in advance to constrain their values to a more proper range. In the general situation, values of  $\alpha$  and  $\beta$  are less than 0.1 and bigger than 0. Further investigation may be conducted by incorporating well log data information into constructing a more comprehensive objective function, in that case direct inversion may be carried out. Numerical simulations demonstrate that the proposed double parameterized regularization inversion method possesses attractive property in efficiency, stability and accuracy, and has potential applications in tackling a huge amount of manual velocity model building problems.

## ACKNOWLEDGEMENTS

We acknowledge the reviewers' and the editor's very helpful comments on improvement of our paper. We thank Pavel Golikov's and Debashish Sarkar's kind suggestions on algorithmic discussions. We are also grateful to Professor Zuhair Nashed for his technical discussions. We acknowledge the Center for Wave Phenomena (CWP) for supplying SU codes for the synthetic seismograms. This work is supported by the National Natural Science Foundation of China under grant numbers 41325016, 11271349, R & D of Key Instruments

and Technologies for Deep Resources Prospecting (the National R & D Projects for Key Scientific Instruments) under grant number ZDYZ2012-1-02-04 and National Science and Technology Major Project 2011zx05008-006-02-01.

## REFERENCES

- Adler F., Baina R., Soudani M.A., Cardon P. and Richard J.-B. 2008. Nonlinear 3D tomographic least-squares inversion of residual moveout in Kirchhoff prestack-depth- migration common-image gathers. *Geophysics* **73**, VE13–VE23.
- Alkhalifah T. 1995. Efficient synthetic - seismogram generation in transversely isotropic, inhomogeneous media. *Geophysics* **60**, 1139–1150.
- Alkhalifah T. 1997. Seismic data processing in vertically inhomogeneous TI media. *Geophysics* **62**, 662–675.
- Alkhalifah T. and Tsvankin I. 1995. Velocity analysis for transversely isotropic media. *Geophysics* **60**, 1550–1566.
- Alkhalifah T., Fomel S. and Biondi B. 2001. The space-time domain: theory and modelling for anisotropic media. *Geophysical Journal International* **144**, 105–113.
- Behera L. and Tsvankin I. 2009. Migration velocity analysis for tilted transversely isotropic media. *Geophysical Prospecting* **57**, 13–26.
- Berkhout A.J. 1997. Pushing the limits of seismic imaging, Part II: Integration of prestack migration, velocity estimation and AVO analysis. *Geophysics* **62**, 954–969.
- Biloti R., Santos L.T. and Tygel M. 2002. Multiparametric traveltimes inversion. *Studia Geophysica et Geodaetica*. **46**, 177–192.
- Charles S., Mitchell D., Holt R., Lin J. and Mathewson J. 2008. Data-driven tomographic velocity analysis in tilted transversely isotropic media: A 3D case history from the Canadian Foothills. *Geophysics* **73**, VE261–VE268.
- Costa J.C., Silva F. J. C., Gomes E. N. S., Schleicher J., Melo L. A. V. and Amazonas D. 2008. Regularization in slope tomography. *Geophysics* **73**, VE39–VE47.
- Fletcher R. 1987. *Practical Methods of Optimization*. Jon Wiley and Sons, Chichester.
- Grechka V. and Tsvankin I. 1999. 3-D moveout inversion in azimuthally anisotropic media with lateral velocity variation: Theory and a case study. *Geophysics* **64**, 1202–1218.
- Grechka V., Pech A. and Tsvankin I. 2002. P-wave stacking-velocity tomography for VTI media. *Geophysical Prospecting* **50**, 151–168.
- Li Y. and Biondi B. 2011. Migration velocity analysis for anisotropic models. *SEG Technical Program Expanded Abstracts*, 201–206.
- Liu M.C. 2010. An application case study for anisotropic velocity analysis (in Chinese). *Oil Geophysical Prospecting* **45**, 525–529.
- Liu Z. 1997. An analytical approach to migration velocity analysis. *Geophysics* **62**, 1238–1249.
- Liu Z. and Bleistein N. 1995. Migration velocity analysis-theory and an iterative algorithm. *Geophysics* **60**, 142–153.

- Sarkar D. and Tsvankin I. 2003. Analysis of image gathers in factorized VTI media. *Geophysics* **68**, 2016–2025.
- Sarkar D. and Tsvankin I. 2004. Migration velocity analysis in factorized VTI media. *Geophysics* **69**, 708–718.
- Sava P. and Vlad I. 2008. Numeric implementation of wave-equation migration velocity analysis operators. *Geophysics* **73**, VE145–VE159.
- Stork C. 1992. Reflection tomography in the postmigrated domain. *Geophysics* **57**, 680–692.
- Thomsen L. 1986. Weak elastic anisotropy. *Geophysics* **51**, 1954–1966.
- Tsvankin I. 2001. *Seismic Signatures and Analysis of Reflection Data in Anisotropic Media*. Elsevier.
- Tsvankin I. and Thomsen L. 1994. Nonhyperbolic reflection moveout in anisotropic media. *Geophysics* **59**, 1290–1304.
- Wang X.X. and Tsvankin I. 2011. Ray-based gridded tomography for tilted TI media. SEG Annual Meeting, San Antonio, USA, 237–242.
- Wang Y.F. 2007. *Computational Methods for Inverse Problems and Their Applications* (in Chinese). Higher Education Press, Beijing.
- Wang Y.F., Yang C.C. and Duan Q.L. 2009. On iterative regularization methods for migration deconvolution and inversion in seismic imaging (in Chinese). *Chinese Journal of Geophysics*. **52**, 1615–1624
- Wang Y.F., Stepanova I. E., Titarenko V. N. and Yagola A. G. 2011a. *Inverse Problems in Geophysics and Solution Methods*. Higher Education Press, Beijing.
- Wang Y.F., Yagola A.G. and Yang C.C. (eds). 2011b. *Optimization and Regularization for Computational Inverse Problems and Applications*. Springer, Berlin.
- Weibull W. and Arntsen B. 2012. Anisotropic migration velocity analysis using the elastic wave equation. 74th EAGE Conference, Copenhagen, Denmark, Expanded Abstract.
- Woodward M.J., Nichols D., Zdraveva O., Whitfield P. and Johns T. 2008. A decade of tomography. *Geophysics* **73**, VE5–VE11.
- Yilmaz O. and Chambers R. 1984. Migration velocity analysis by wavefield extrapolation. *Geophysics* **49**, 1664–1674.
- Yuan Y.X. and Sun W.Y. 1997. *Optimization Theory and Methods* (in Chinese). Science Press, Beijing.
- Zhang H.B. and Yang, C.C. 2003. A constrained impedance inversion method controlled by regularized parameters (in Chinese). *Chinese Journal of Geophysics* **46**, 827–834.
- Zhou H.B., Guo J. and Young J. 2001. An alternative residual-curvature velocity updating method for prestack depth migration. 71<sup>st</sup> Annual International SEG Meeting, San Antonio, USA, Expanded Abstracts, 877–880.

## APPENDIX

### QUASI-NEWTON FORMULAE

The quasi-Newton method for a general non-linear minimization problem (Yuan and Sun 1997)

$$\min f(\mathbf{x}), \quad \mathbf{x} \in X, \quad (\text{A1})$$

refers to the following iterative formula: for  $k = 1, 2, \dots$ ,

$$\begin{cases} \mathbf{g}_k = \nabla f(\mathbf{x}_k), \\ \mathbf{d}_k = -\mathbf{B}_k \mathbf{g}_k, \\ \mathbf{x}_{k+1} = \mathbf{x}_k + \omega_k \mathbf{d}_k, \\ \omega_k \text{ obtained by line search,} \\ \mathbf{y}_k = \mathbf{g}_{k+1} - \mathbf{g}_k, \\ \mathbf{s}_k = \mathbf{x}_{k+1} - \mathbf{x}_k, \\ \mathbf{B}_{k+1} \mathbf{y}_k = \mathbf{s}_k. \end{cases} \quad (\text{A2})$$

To use the quasi-Newton method, the quasi-Newton condition

$$\mathbf{B}_{k+1} \mathbf{y}_k = \mathbf{s}_k, \quad (\text{A3})$$

must be satisfied. A popular formula for updating  $\mathbf{B}_k$  is given by the Broyden-Fletcher-Goldfarb-Shanno (BFGS) method, given by

$$\begin{cases} \mathbf{B}_{k+1} = \mathbf{V}_k^T \mathbf{B}_k \mathbf{V}_k + \rho_k \mathbf{s}_k \mathbf{s}_k^T, \\ \rho_k = \frac{1}{\mathbf{y}_k^T \mathbf{s}_k}, \\ \mathbf{V}_k = \mathbf{I} - \rho_k \mathbf{y}_k \mathbf{s}_k^T. \end{cases} \quad (\text{A4})$$

Recalling our objective function is a non-linear function  $J^{\alpha, \beta}(\Delta\lambda)$  (see equation (3)), the gradient of  $J^{\alpha, \beta}$  can be evaluated as

$$\begin{aligned} g(\Delta\lambda) &= \frac{d}{d\Delta\lambda} J^{\alpha, \beta}(\Delta\lambda) = \frac{1}{2} \frac{d}{d\Delta\lambda} \|\mathbf{A}\Delta\lambda + \mathbf{b}\|^2 \\ &\quad + \frac{\beta}{2} \frac{d}{d\Delta\lambda} \|\Delta\lambda - \Delta\lambda^0\|^2 \\ &\quad + \alpha \frac{d}{d\Delta\lambda} \Omega(\Delta\lambda). \end{aligned} \quad (\text{A5})$$

Since

$$\begin{aligned} \|\mathbf{A}\Delta\lambda + \mathbf{b}\|^2 &= (\mathbf{A}\Delta\lambda + \mathbf{b}, \mathbf{A}\Delta\lambda + \mathbf{b}), \\ \|\Delta\lambda - \Delta\lambda^0\|^2 &= (\Delta\lambda - \Delta\lambda^0, \Delta\lambda - \Delta\lambda^0), \\ \Omega(\Delta\lambda) &= \sum_i h_{\bar{\epsilon}}(\Delta\lambda_i), \end{aligned}$$

taking derivatives of the above three functions about  $\Delta\lambda$  yields

$$g(\Delta\lambda) = \mathbf{A}^T(\mathbf{A}\Delta\lambda + \mathbf{b}) + \alpha K(\Delta\lambda) + \beta(\Delta\lambda - \Delta\lambda^0), \quad (\text{A6})$$

as  $K(\Delta\lambda)$  is given by

$$K(\Delta\lambda) = \left[ \frac{\partial \Omega}{\partial \Delta\lambda_1}, \dots, \frac{\partial \Omega}{\partial \Delta\lambda_p} \right]^T,$$

and  $\frac{\partial \Omega}{\partial \Delta \lambda_i} = \sum_i h_{i\bar{\varepsilon}}(\Delta \lambda_i)$ . Thus the following equations will be used during iteration

$$\begin{cases} \mathbf{g}_k = g(\Delta \lambda_k), \\ \mathbf{d}_k = -\mathbf{B}_k \mathbf{g}_k, \\ \Delta \lambda_{k+1} = \Delta \lambda_k + \omega_k \mathbf{d}_k, \\ \omega_k \text{ obtained by line search} \end{cases} \quad (\text{A7})$$

and  $\mathbf{B}_k$  is updated using equations (A4). For implementation of the quasi-Newton method, one has to solve  $\omega_k$  using some line search techniques. This requires

solving a non-linear one-dimensional (1D) minimization problem

$$\omega_k = \arg \min_{\omega} J^{\alpha, \beta}(\Delta \lambda_k + \omega \mathbf{d}_k). \quad (\text{A8})$$

We can solve equation (A8) exactly or approximately. Since  $\omega_k$  is a trial step in each iteration, it is unnecessary to solve it exactly. There are many useful inexact line search methods, for example Wolfe line search (see equations (6) and (7)), Armijo-Goldstein criterion, Powell line search, and so on (Fletcher 1987; Yuan and Sun 1997).